

RESEARCH

Open Access



# Nanoelectronic COupled Problems Solutions: uncertainty quantification for analysis and optimization of an RFIC interference problem

Piotr Putek<sup>1,2\*</sup> , Rick Janssen<sup>3</sup>, Jan Niehof<sup>3</sup>, E. Jan W. ter Maten<sup>1</sup>, Roland Pulch<sup>2</sup>, Bratislav Tasić<sup>3</sup> and Michael Günther<sup>1</sup>

\*Correspondence:

[Putek@math.uni-wuppertal.de](mailto:Putek@math.uni-wuppertal.de)

<sup>1</sup>Bergische Universität Wuppertal, Wuppertal, Germany

<sup>2</sup>Ernst-Moritz-Arndt-Universität Greifswald, Greifswald, Germany  
Full list of author information is available at the end of the article

## Abstract

The FP7 project nanoCOPS (the 7th Framework Programme project Nanoelectronic COupled Problems Solutions) derived new methods for simulation during development of designs of integrated products. It has covered advanced simulation techniques for electromagnetics with feedback couplings to electronic circuits, heat and stress. It was inspired by interest from semiconductor industry and by a simulation tool vendor in electronic design automation.

Due to the application of higher frequencies and the continuous down-scaling process, there is a higher probability of unforeseen interactions between different domains of a Radio Frequency Integrated Circuit (RFIC), which can lead to the variability of the output performance functions. Since these undesired phenomena ought to be investigated in the early phases of the integrated circuit (IC) design, in this work we formulate the robust optimization problem in terms of the expectation and the standard deviation values under the uncertainties of material parameters.

Therein, the statistical information included in the multi-objective functional can be provided by a response surface model. For this purpose the Stochastic Collocation Method (SCM) combined with Polynomial Chaos Expansion (PCE) has been used. The reason for analyzing the variability of the Electromagnetic Interference (EMI) is, on the one hand, to quantify the uncertainty in an integrated Radio-Frequency Complementary Metal-Oxide Semi-Conductor (RFCMOS) transceiver design, and, on the other hand, to improve this design in a robust sense. We have illustrated our methodology for an integrated Radio-Frequency Complementary Metal-Oxide Semi-Conductor (RFCMOS) transceiver design.

**Keywords:** Floor-plan modeling; Isolation grounding; Polynomial chaos expansion; Stochastic collocation method; Uncertainty quantification; Robust design optimization; Sobol decomposition; Variance-based and local sensitivity analysis

## 1 Introduction

Nowadays the computational electromagnetic (CEM) modeling methods are the integral part of the advanced tools for electromagnetic compatibility (EMC) problems of integrated circuits (ICs), encountered in engineering practice [2]. In contrast to the tradi-

tional EMC product testing, which are both time-consuming and expensive, computational modeling and simulation offer more flexibility in design modification and are potentially faster and cheaper [39]. They can be applied to resolve a broad range of real life problems, including interference issues and coupling effects in modern mixed-signal and radio frequency integrated circuits. The latter has become more and more important with the continuous integration process of RF, mixed signal and digital blocks on a single die, which is additionally combined with observable trends on semiconductor market to apply higher frequencies for accommodating higher data rates [20]. These trends towards miniaturization of RFIC allows primarily for easier implementation of multiple functions in a compact unit, which implies also substantial reductions in product cost. In fact, the complexity poses many challenges in the integration process of various subsystems, such as the so-called aggressors (the noisy blocks), the victims (the sensitive part, affected by noise) and other intellectual property (IP) blocks to ensure their proper and interference-free operation [15]. Additionally, provisions should be made at the influence of the miniaturization on the failure probability associated with yield loss due to defects, faults, process variations and design issues [37]. In fact, the statistical variations in input parameters, originating from manufacturing tolerances of industrial processes, may result in a thermal destruction of devices due to thermal runaway [30, 32]. In this respect, taking the input statistical variations into account in modeling allows for providing the predictable and reliable RFIC simulations. Moreover, unintended RF coupling, caused by industrial imperfections and miniaturization due to the scaling-down process, could significantly downgrade the quality of products and their performance or even be dangerous for safety of both environment and the end-users [8]. Thus, to meet the stringent design specification requirements for electromagnetic compatibility standards [4] such as speeds, bandwidth, noise margin crosstalk, etc., the ICs designers have to be aware of interference issues caused by high-frequency phenomena and randomness involved in the manufacturing process. Considering these phenomena at early design stages allows for avoiding expensive re-spins and to reduce iterations in the time-to-market cycle.

Therefore, the structured methodology is needed to model the adverse effects caused by the manufacturing process using polynomial chaos expansion combined with the stochastic collocation method [43–46] for analysis of the EMC problem of integrated circuits. Here, we focus more on the new application of the methodology mainly developed in [32, 33, 35]. Taking this into account, the special attention is paid to the analysis of both the means of the gradient of the output characteristics with respect to parameter variations and on the variance-based sensitivity, which allows for quantifying impact of particular parameters to the variance of output functions. For this purpose, the Sobol decomposition [38] has been applied. The proposed approach is innovative, since statistics based on uncertainty quantification (UQ) allows for assessing the most influential input random parameter, which can be further used for the physically-based design of RFIC model. Additionally, the UQ can be incorporated in the Gauss-Newton optimization algorithm [27], which yields the powerful tools for the automatic design of RFIC system, while taking both noise and uncertain input parameters into account. More specifically, based on results achieved in [28], the so-called mean gradient sensitivity analysis has been explored to approximate the derivative of the robust functional, which furthermore, has been applied in the optimization process. Hence, the current paper is an extended version of [29]

providing detailed insights on the floorplanning and grounding strategy as well as new results for the variance-based and the local sensitivity analysis.

The paper is organized as follows. Section 2 overviews the methodology developed and used for modeling and simulation of an integrated RFCMOS transceiver for automotive applications, that is the so-called floorplan modeling and isolation strategy. Section 3, in turn, considers the benefits of the PCE-based stochastic collocation methods applied for solving the random-dependent Differential-Algebraic Equations (DAEs) and additionally provides the results for the variance-based and the local sensitivity analysis. Section 4 deals with the robust optimization problem, which definition includes the statistical moments, used as cost functional. Section 5 gives some achievements obtained during the project with respect to reliable RFIC isolation. And finally, in Sect. 6 we briefly summarize our paper including remarks and future work on this research.

## 2 Methodology for deterministic modeling

In this work, we analyze a design of an integrated RFCMOS automotive transceiver design, depicted on Fig. 1, which is treated in our study as a test case. Thus, we consider a fully functional chip [20], which, in particular, is comprised of four main subsystems such as (i) an analog-to-digital converter (ADC), (ii) the receiver and power amplifier (RxPA), (iii) the crystal oscillator and local oscillator (XoLO) and (iv) the digital part. Therein, for the noise generation, which affects proper functioning of other systems, the so-called aggressor units such as digital logic, digital input/output (IO) systems (IOs), clock generation circuits, etc. are responsible. Due to the complexity of the used test case, the proper methodology needs to be used in order to analyze the EMC problems. Within this context, the proper operation of devices and circuits in electromagnetic environment can be achieved by applying appropriate shielding strategy together with controlled low emission of noise sources. Therefore, to take into account varied type of coupling in our modeling approach, the special methodology, proposed in [20] and further developed by [15], has been applied. This methodology makes use of an overall model of the RF product, consisting of the following key elements:

- On-chip: domain-regions, padding, sealing, splitter cells, substrate effects (including deep-Nwell and Pwell regions).

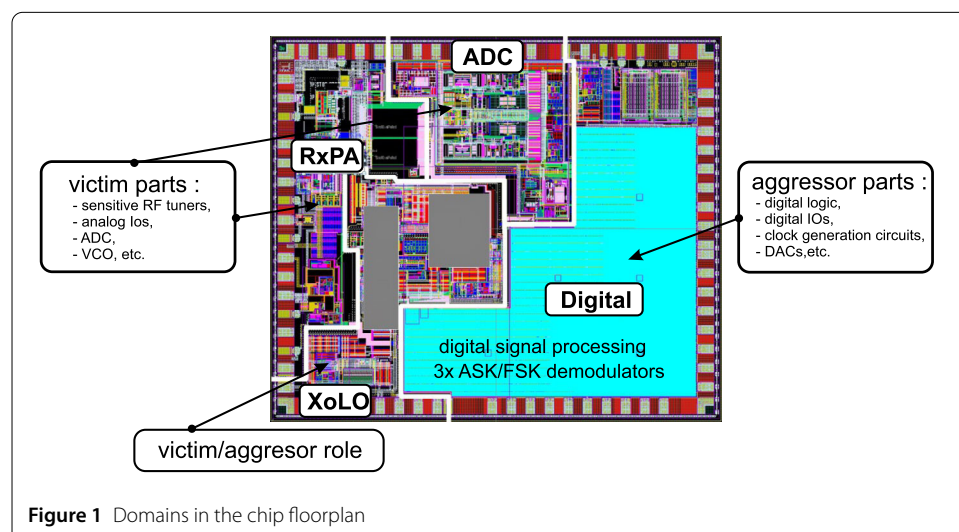


**Figure 1** Domains in the chip floorplan

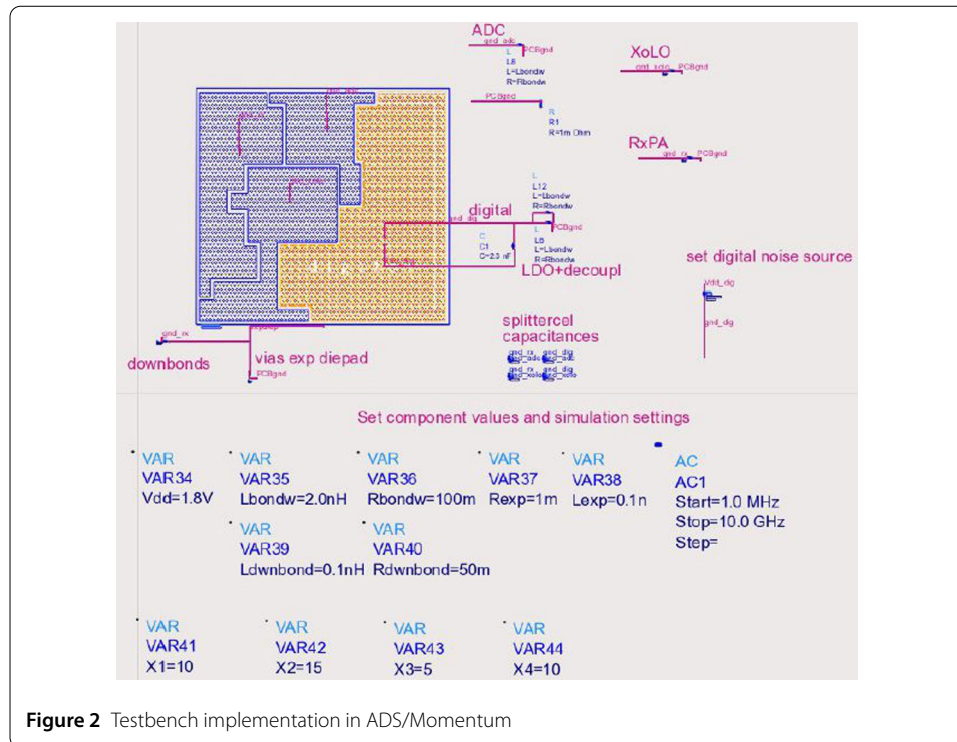


**Figure 2** Testbench implementation in ADS/Momentum

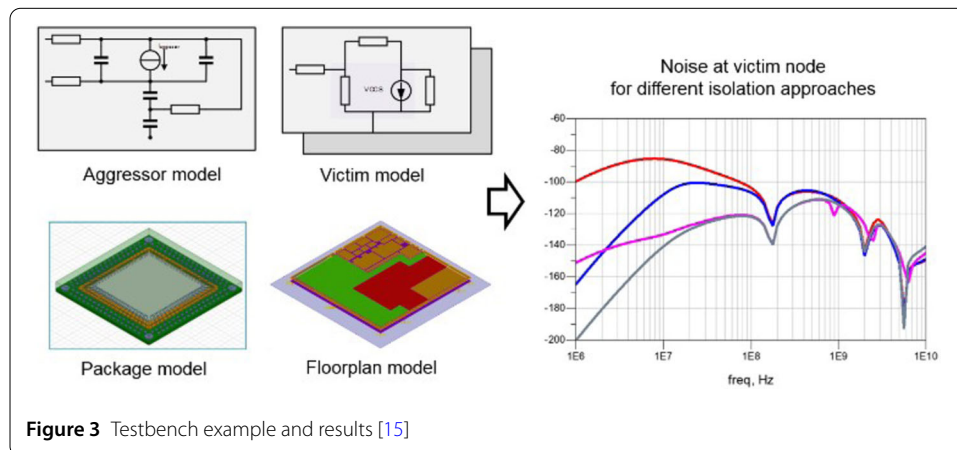


**Figure 3** Testbench example and results [15]

- Package: ground and power pins, bondwires/downbonds, exposed diepad connection.
- Printed Circuit Board (PCB): ground plane and exposed diepad connections.

An abstract, high level simulation model is constructed (see Figs. 2 and 3), connecting the above mentioned key elements together. Noise sources/interferences are supplied to this network of elements. A typical topic of investigation is the isolation of the sensitive RF domain (= ADC + RxPA + XoLO) with respect to the noise coming from the digital domain. Physical implementation parameters of interests are then a.o., the number of downbonds, the number of ground pins, domain spacing, domain shape, application of deep-Nwell, exposed diepad, the number of exposed diepad vias. In the specific case of the development of the transceiver IC a key requirement is isolation of the (very) sensitive, single-ended receiver block from the 'dirty' digital part. This is essential to ensure product compliance with specifications.

## 2.1 Mathematical modeling for an RFCMOS automotive test case

In our work, to avoid computationally expensive simulations of the fully three-dimensional model of RFIC [39, 48], the Equivalent Circuit Model (ECM) with the appropriate floor-plan modeling and isolation strategy has been used. More specifically, the ECM has been created based on the simulation of a chip architecture using the Advanced Design System (ADS)/Momentum software from Keysight Technologies [18]. Hence, for the solution of systems of partial differential equations the Methods of Moments (MoM) [6] has been employed, where the concept of Green functions is explored to model the proper behavior of the substrate [12].

Therein, the interaction of the ICs with their physical environment has been considered by solving an integral formulation of the time-harmonic partial differential equations (PDEs), derived from Maxwell's equations

$$\nabla \cdot \epsilon(\theta) [\nabla V(\theta) + i\omega \mathbf{A}(\theta)] = -\tilde{\rho}(\theta), \quad (1a)$$

$$\nu(\theta) \nabla \times \nabla \times \mathbf{A}(\theta) = \mathbf{J}(\theta) + \omega^2 \epsilon(\theta) \left[ \mathbf{A}(\theta) - i \frac{\nabla V(\theta)}{\omega} \right], \quad (1b)$$

$$\nabla \cdot \mathbf{A}(\theta) + i\omega k V(\theta) = 0, \quad (1c)$$

$$\nabla \cdot \mathbf{J}(\theta) + i\omega \tilde{\rho}(\theta) = 0, \quad (1d)$$

which have been equipped with suitable initial and boundary conditions, in the commercial software Momentum [18]. Here, the variable  $i$  is defined by  $i = \sqrt{-1}$ ,  $k$  denotes a scaling factor, while  $\tilde{\rho}$  is the charge density. In the above system (1a)–(1d),  $V$  denotes the electric scalar potential, while  $\mathbf{A}$  is the magnetic vector potential. The location in space is denoted by  $\mathbf{r}$  and  $\theta := (\mathbf{r}, f)$ ;  $\omega = 2\pi f$  refers to the angular velocity with  $f$  being the frequency. The real-valued functions  $\epsilon(\mathbf{r})$  and  $\nu(\mathbf{r})$  describe the permittivity and the reluctivity, respectively. We have carried out our simulations in a time-harmonic regime that yields accurate electromagnetic simulation performance at radio frequencies for the geometrically complex and electrically small designs. Their outcome in the form of S-parameters, generated for general planar circuits, contains sufficient amount of information in order to characterize each individual component, used in the ECM. The ADS tool of Momentum, which is advantageous in describing the electrical device characteristics, gives the opportunity to model the behavior of RF passive component by a frequency independent lumped model [18]. Thus, this lumped model can be further explored in both the direct and optimization problems [28, 29].

For this purpose, based on the conducted simulations of (1a)–(1d) and the proper floor-planning with grounding strategies, an equivalent circuit model of the IC and package has been developed [20], depicted in Fig. 2. It is supposed to be the lumped model of the 3D model, shown in Fig. 1. When for the mathematical modeling of the EMC the flux/charge oriented Modified Nodal Analysis (MNA) has been used, the time-harmonic structured DAE, written in a compact way, is given by

$$i\omega \mathbf{C}(\mathbf{p}^{(k)}) \mathbf{x}(\mathbf{p}^{(k)}, f) + \mathbf{G}(\mathbf{p}^{(k)}) \mathbf{x}(\mathbf{p}^{(k)}, f) = \mathbf{s}(f), \quad k = 1, \dots, K, \quad (2)$$

where  $\mathbf{x}(\mathbf{p}, f) \in \mathbb{C}^n$  denotes the vector of unknowns, which contain node voltages, independent and dependent voltage source currents as well as inductor currents;  $\mathbf{p}$  is the pa-



parameter of interest.  $\mathbf{s}(f) \in \mathbb{C}^n$  refers to an input vector which is determined by the independent current and voltage sources. The matrices  $\mathbf{C}(\mathbf{p}), \mathbf{G}(\mathbf{p}) \in \mathbb{C}^{n \times n}$  describe the lumped memory-less and memory elements, respectively, which depend only on the parameters  $\mathbf{p}$ , while  $n$  corresponds to the total number of MNA variables [11, 13, 36].

Specifically, in our work we are particularly interested in how the digital domain influences other subsystems. To this end, we define for a (scalar) cross-domain coupling the transfer function as in [5]

$$G(\omega) = \frac{|Y|}{|X|} =: |H(i\omega)|, \quad \phi(\omega) := \phi_Y - \phi_X = \arg(H(i\omega)), \quad (3)$$

when considering a complex harmonic system with a sinusoidal component of  $|X|$ , an angular frequency  $\omega$  and a phase  $\phi := \arg(X)$  as an input to a linear time-invariant system and then its corresponding output as  $|Y|$  and  $\phi_Y := \arg(Y)$ . The specific definitions of objective functions to be included in the optimization procedure will be given in Sect. 4.1. More information on the extraction of the equivalent circuit model from the PDEs can be found, e.g., in [15, 20]. For the needs of this study, we also briefly recall some basic concepts of the EMC extraction that are required for stochastic modeling. It will be a topic of Sects. 2.2 and 2.3.

## 2.2 Testbench model of the integrated circuit

As the first step, an initial floorplan model, describing the interaction between individual IP blocks/substrate domains via the substrate and well structures, is created. If present, also the connection of the backside of the die is included by taking the vertical substrate noise propagation path into account. Each IP block is represented by a single port, representing substrate connections. Such a first-order model can be created with a number of commercially available EM simulators. Initially, a rough estimate of the technology parameters can be sufficient (e.g., substrate conductivity). The output (either S-parameters or lumped circuit components) is then included in the simulation testbench shown later. In addition in finding the optimal relative placement of the IP blocks and the spacing between them, this model can also be used to study the impact of, e.g., type of substrate (bulk vs. silicon-on-insulator), doping levels (lowly-doped vs. highly-doped), backside connection (soldered vs. glued), etc. Figure 3 shows an example floorplan model indicating the typical complexity (number of used substrate/ground domains) of the analyzed design.

The aggressor current, representing the switching activity of, e.g., the digital block, produces a bounce on the supply and ground nodes due to the finite impedance of the supply/ground network. This noise then couples to the victim through the substrate represented by the floorplan model. The values of the well junction capacitances representing the well structures are determined by the technology, the aggressor area and the design style (e.g., presence of Deep N-Well). In addition, currents through the bondwires can also inductively couple to the bondwires of the victim circuit. On-chip voltage regulators and decoupling capacitances have an impact on the coupling and need to be included in the model, either as S-parameters or by a simplified circuit model. Typical aggressors include: digital logic, digital IOs, clock generation circuits, a digital-to-analog converter (DAC) and ADC.

When more details about the victim IP architecture become available, a simple victim circuit can be created. For example, a low-noise amplifier can be represented by a voltage-

controlled current source, or an ideal operational amplifier with a simplified feedback circuit. In this case, in addition to the substrate noise rejection properties of the circuit, the noise coupling to the amplifier input can be included in the model. Finally, when the design of the victim block is complete, an S-parameter file, containing the relevant terminals (e.g. substrate and sensitive input), should be generated by the IP designer for inclusion in the interference testbench. Typical victims are: sensitive RF tuners, analog IOs, ADC, voltage controlled oscillators (VCO), etc.

Similar to victim IP models, different levels of abstraction are used to incorporate the package coupling effects in the analysis. Again, at early stages, a very simple model could be useful. Lumped inductances with estimated values based on expected lengths of bond-wires [3] and leads are added to the testbench. Later, it can be extended with estimates of mutual inductances and capacitances, based on previous designs or simple models. At this stage, a concurrent optimization of the floorplan and the IO ring takes place. Finally, when the IO ring and pin assignment is fixed and the package choice is finalized, the full-package model can be included in the test bench for a more accurate prediction of inductive and capacitive effects. The models of individual IP blocks, the floorplan and the package are combined in a single testbench, which is used to investigate the total effect of all implemented isolation measures (see Fig. 3).

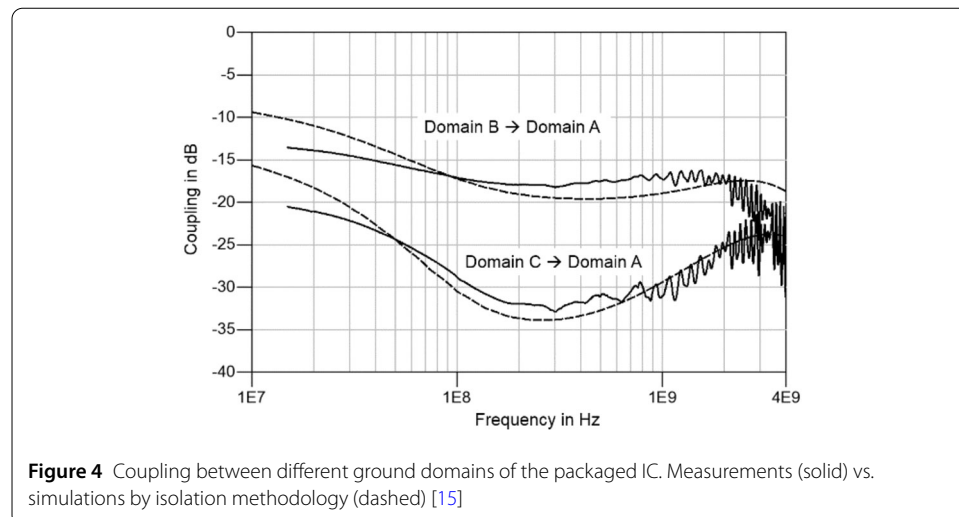
### 2.3 Verification of the applied methodology

Validation of the methodology has been reported in [20]. The same relative effect of 8–9 [dB] by adding the downbonds for the ground connections has been observed in both simulated transfer values, as well as in spur measurements of packaged IC samples.

A more direct validation approach includes comparison of the voltage transfer between different ground domains in the design. As can be seen from Fig. 4, the general trends are predicted within a few [dB] for various combinations, indicating that the main coupling paths, as well as the parameter estimates, are properly incorporated in the model [15].

### 3 Stochastic modeling and uncertainty quantification

In the model (2), we replace physical parameters  $\mathbf{p} \in \Pi \subseteq \mathbb{R}^q$  by independent random variables  $\mathbf{p} : \Omega_{\text{pr}} \rightarrow \Pi$  on some probability space  $(\Omega_{\text{pr}}, \mathcal{A}, \mathbb{P})$  to quantify uncertainties. Let  $p_i$



for  $i = 1, \dots, q$  be a random variable with a traditional probability distribution like uniform distribution or Gaussian distribution, for example. The solution of the system (2) becomes a random field, i.e., each component of the solution represents a function depending on the random variables  $\mathbf{p}$  for fixed frequency  $f \in \mathcal{F}$  in some frequency range  $\mathcal{F} \subseteq \mathbb{R}$ . The chosen physical parameters belong to the four different parts (a)–(d) of the functional chip specified in Sect. 2.1.

### 3.1 Polynomial chaos expansion

Let  $z : \Pi \rightarrow \mathbb{R}$  be a measurable function depending on the random variables. The associated expected value reads as

$$\mathbb{E}[z] = \int_{\Omega_{\text{pr}}} z(\mathbf{p}(\chi)) \, d\mathbb{P}(\chi) = \int_{\Pi} z(\mathbf{p}) \rho(\mathbf{p}) \, d\mathbf{p} \quad (4)$$

using the probability density function  $\rho : \Pi \rightarrow \mathbb{R}$ . The variance is defined as usual by  $\text{Var}[z] = \mathbb{E}[(z - \mathbb{E}[z])^2]$ . A function  $z$  is square-integrable, if the expected value  $\mathbb{E}[z^2]$  exists. Moreover, it holds that  $\mathbb{E}[\Phi_i \Phi_j] = \delta_{ij}$  with the Kronecker delta symbol.

Any square-integrable function owns a unique Polynomial Chaos (PC) expansion, see [44]. Let  $y : \Pi \times \mathcal{F} \rightarrow \mathbb{R}$  be a function depending on the domain  $\mathcal{F}$  as well as the random variables in  $\Pi$ . If  $y$  is always square-integrable with respect to the random variables, it holds that

$$y(\mathbf{p}, f) = \sum_{i=0}^{\infty} v_i(f) \Phi_i(\mathbf{p}) \quad \text{for each } f \quad (5)$$

with the coefficients  $v_i : \mathcal{F} \rightarrow \mathbb{R}$  and the basis polynomials  $\Phi_i : \Pi \rightarrow \mathbb{R}$ . Moreover, it holds that  $\mathbb{E}[\Phi_i \Phi_j] = \delta_{ij}$  with the Kronecker delta symbol. The convergence is in the mean-square sense in the probability space. The coefficients become frequency-dependent functions and are defined by the inner products

$$v_i(f) = \mathbb{E}[y(\cdot, f) \Phi_i(\cdot)] \quad \text{for } i \in \mathbb{N}_0 \text{ and each } f. \quad (6)$$

Consequently, we consider the PC expansion (5) pointwise in the frequency parameter.

In practice, just a finite number of terms can be handled, which implies a truncated expansion

$$\tilde{y}(\mathbf{p}, f) = \sum_{i=0}^N v_i(f) \Phi_i(\mathbf{p}) \quad \text{for each } f \quad (7)$$

as an approximation of the exact function (5). Often all polynomials up to some total degree  $d$  are included. Since  $q$  independent random variables are given, the number of basis polynomials becomes  $N + 1 = \frac{(d+q)!}{d!q!}$ . Furthermore, assuming that  $\Phi_0 = 1$ , the expected value and the variance are given by

$$\mathbb{E}[y(\cdot, f)] \doteq \mathbb{E}[\tilde{y}(\cdot, f)] = v_0(f) \quad \text{and} \quad \text{Var}[y(\cdot, f)] \doteq \text{Var}[\tilde{y}(\cdot, f)] = \sum_{i=1}^N |v_i(f)|^2 \quad (8)$$

when using (7).



### 3.2 Pseudo-spectral approach

In our work, we apply a stochastic collocation method for the approximation of the coefficient functions in the truncated expansion (7). Therein, the probabilistic integrals (4) in (6) are computed approximately by a multidimensional quadrature rule, which is specified by a set of nodes  $\{\mathbf{p}^{(1)}, \dots, \mathbf{p}^{(K)}\} \subset \Pi$  and a set of weights  $\{w_1, \dots, w_K\} \subset \mathbb{R}$ . Thus, the approximations read as

$$\tilde{v}_i(f) = \sum_{k=1}^K w_k y(\mathbf{p}^{(k)}, f) \Phi_i(\mathbf{p}^{(k)}) \quad \text{for each } f \quad (9)$$

and  $i = 0, 1, \dots, N$ . Specifically, the Stroud formula of order 3, see [30, 32], is used in a numerical quadrature. The number of nodes becomes  $K = 2q$ , which is the minimum number required for a polynomial exactness of degree 3. The associated weights are all positive and identical, i.e.,  $w_k = \frac{1}{2q}$  for all  $k$ , which represents an advantageous property with respect to error propagation. In our application, we consider the solution of the model (2) with random parameters. Thus, the evaluation of (9) requires the numerical solution of  $K$  deterministic systems (2) including boundary conditions, one system for each parameter realization.

### 3.3 Sobol decomposition and variance-based sensitivity analysis

Given a function  $z : \Pi \rightarrow \mathbb{R}$  depending on parameters  $\mathbf{p}$ , we are interested in sensitivities. Local sensitivities are given by the partial derivatives of the deterministic parameter-dependent function  $z$  provided that the function is smooth.

Global sensitivities quantify the dependence on the random variables  $\mathbf{p}$  in the probability space. The global sensitivity coefficients can be defined by the PC expansion of a square-integrable random variable, see [24, 25, 38]. We define the index sets

$$\mathcal{I}_j = \{i \in \mathbb{N}_0 : \Phi_i \text{ is non-constant in } p_j\} \quad \text{for } j = 1, \dots, q,$$

which represent the sets of polynomials depending on a particular random variable. Let  $(v_i)_{i \in \mathbb{N}_0}$  be the PC coefficients of the function  $z$ . A truncation of the index sets and the approximation (8) of the variance generate an approximation of the global sensitivity coefficients, i.e.,

$$S_j = \left( \sum_{i \in \tilde{\mathcal{I}}_j} v_i^2 \right) / \left( \sum_{i=1}^N v_i^2 \right) \quad \text{for } j = 1, \dots, q \quad (10)$$

with finite index sets  $\tilde{\mathcal{I}}_j = \mathcal{I}_j \cap \{0, 1, \dots, N\}$ . These approximations implies the bounds

$$0 \leq S_j \leq 1 \quad \text{for each } j \quad \text{and} \quad 1 \leq S_1 + S_2 + \dots + S_q \leq q. \quad (11)$$

A random variable  $p_j$  exhibits a relatively strong impact on the output  $z$ , if it holds that  $S_j \approx 1$ . If  $S_j \approx 0$ , it is not significant. In our application, a function  $y : \Pi \times \mathcal{F} \rightarrow \mathbb{R}$  is given. Thus, we apply the above approach pointwise for  $f \in \mathcal{F}$ . The total effect sensitivity coefficients (10) become functions  $S_j : \mathcal{F} \rightarrow \mathbb{R}$  for  $j = 1, \dots, q$ . The SCM yields approximations (9) of the coefficient functions, which can be inserted in (10). Hence, our numerical approach yields the global sensitivities without additional computational work.

Moreover, differentiating (7) with respect to  $p_j$  yields  $\partial \tilde{y} / \partial z_j$  at any value of  $\mathbf{z}$  defined as

$$\left. \frac{\partial \tilde{y}}{\partial z_j} \right|_{z_j = \bar{z}_j} = \sum_{n=0}^N v_n \frac{\partial \Phi_n}{\partial z_j} \frac{\partial \mathbf{z}}{\partial p_j}, \quad j = 1, \dots, q. \quad (12)$$

The  $z_j$ th mean sensitivity is obtained by integrating over the whole parameter space [44].

#### 4 Optimization under noise emission and uncertainties

The problem of the empirical design of the cross-domain coupling on RFIC under uncertainties based on the Sobol decomposition [38] has been carried out in paper [48]. Within the nanoCOPS project (<http://fp7-nanocops.eu/>), the variance-based and the local sensitivity analysis based on the PCE surface response model and the adjoint variable method has been explored in many engineering fields. For instance, in [29] the forward stochastic problem of the RFIC isolation under uncertainties has been studied in [28]. In works [30–32], in turn, the PCE-based stochastic collocation methods has been applied for the UQ analysis and the robust shape/topology optimization of the power transistor device under material and geometric uncertainties. Additionally, in the paper [23] the stochastic inverse problem has been investigated. Here, we focus mainly on presenting the robust framework, tailored for the application of the electromagnetic interference variability on the RFIC, which is partially based on the preliminary results achieved in [29].

##### 4.1 Objectives

In the ECM, the activity of the digital domain is represented by a current source  $I_{\text{core}}$ , which acts as an aggressor, shown on Fig. 6. To investigate the impact of noise generated by the aggressor on victims part such as RxPA, XoLO and ADC, based on (3) and under assumption of the first approximation by means of two-ports consisted of  $R, L$  elements, the cross-coupling functions are defined as the frequency response in the following form

$$y_1(\mathbf{p}, f) = |\text{CplADC}(\mathbf{p}, f)| := 20 \log \frac{|\text{gnd\_adc} - \text{PCBgnd}|}{|\text{Vdd\_dig} - \text{gnd\_dig}|}, \quad (13a)$$

$$y_2(\mathbf{p}, f) = |\text{CplXolo}(\mathbf{p}, f)| := 20 \log \frac{|\text{XOLO}_{\text{gnd}} - \text{PCBgnd}|}{|\text{Digital}_{\text{Vdd}} - \text{Digital}_{\text{gnd}}|}, \quad (13b)$$

$$y_3(\mathbf{p}, f) = |\text{CplRx}(\mathbf{p}, f)| := 20 \log \frac{|\text{RxPA}_{\text{gnd}} - \text{PCBgnd}|}{|\text{Digital}_{\text{Vdd}} - \text{Digital}_{\text{gnd}}|}. \quad (13c)$$

These functions allow for measuring the influence of emitted noise into the functioning of RxPA, XoLO and ADC subsystems.<sup>a</sup> Additionally, the respecting bondwires, downbonds and diepad vias, shown on Fig. 6, are assumed to be random-dependent in our stochastic approach, i.e.,  $\mathbf{z}(\mathbf{p}) = (z_1(p_1), z_2(p_1), z_3(p_1), z_4(p_1))^T$ . Because of the application of the time-harmonic analysis, the particular random parameters are represented by impedances  $z_j$ , which are explained more precisely in Sect. 5.

Correspondingly, the cross-coupling functions are the perfect candidates to be considered as the objective functions in the proposed optimization procedure. In our approach, we simply convert the multi-objective optimization problem into the single objective by using the averaged wighted method [17]. Thus, the random-dependent functional is for-

mulated as follows

$$\mathcal{J}(\mathbf{p}, f) = \frac{1}{2} \sum_{i=1}^3 w_i |y_i(\mathbf{p}, f)|^2, \quad (14)$$

where the prescribed weight are assumed to be defined as  $w_i = 0.5$ ,  $i = 1, \dots, 3$ . However, in practical computation, presented in the next section, the response function  $y_1(\mathbf{p}, f)$  had to be excluded from the optimization due to its totally insensitivity with respect to even the relatively large input variations [29].

## 4.2 Robust formulation

In the conventional optimization, it is assumed, for simplicity, that the parameters of interest are treated as deterministic variables. This, in turn, can lead to an optimal configuration, which is very sensitive to the variation of the nominal parameters [47]. From this perspective, there is a need to take into account uncertainties of material and/or geometric parameters, including excitation term that comes from manufacture imperfection, during the optimization process. To solve this problem, we propose to apply the robust framework [40], invented by the Japanese engineer Taguchi. This allows for providing an optimal design of the RFIC, which is insensitive to variations of random parameters as well as robust versus the noise generated by the aggressors.

In the proposed robust formulation [32, 34, 42], an optimization problem constrained by stochastic DAEs (2) read as

$$\inf_{\mathbf{z}(\mathbf{p})} \mathbb{E}[\mathcal{J}(\mathbf{p}, f)] + \eta \sqrt{\text{Var}[\mathcal{J}(\mathbf{p}, f)]} \quad (15a)$$

$$\text{s.t.} \quad i\omega \mathbf{C}(\mathbf{p}^{(k)}) \mathbf{x}(\mathbf{p}^{(k)}, f) + \mathbf{G}(\mathbf{p}^{(k)}) \mathbf{x}(\mathbf{p}^{(k)}, f) = \mathbf{s}(f), \quad k = 1, \dots, K, \quad (15b)$$

$$\mathbf{z}_{\max_\ell} \leq \mathbf{z}_\ell \leq \mathbf{z}_{\min_\ell}, \quad \ell = 1, \dots, P, \quad (15c)$$

where the expectation value  $\mathbb{E}(\cdot)$  and the variance  $\text{Var}(\cdot)$  are defined by (8) and  $3 \leq \eta \leq 6$  is the prescribed coefficient, e.g. for the six-sigma method  $\eta = 6$  [16];  $\mathbf{z}(\mathbf{p})$  is a vector of optimized parameters, while  $\mathbf{z}_{\max_\ell}$  and  $\mathbf{z}_{\min_\ell}$  denote their box constraints, respectively. In the case of any gradient optimization method used to find the solution of the problem (15a)–(15c), the derivative of the robust functional (15a) is required. The next section includes the brief recall of basic concepts of some ‘deterministic’ sensitivity analysis techniques.

## 4.3 Sensitivity analysis for gradient calculation

The sensitivity analysis allows for investigating the influence of inputs perturbation into the variation of output performance functions, i.e., the tolerance analysis. Its application can be further extended to the problems of network synthesis, which is based on the optimization of the assumed network performance function, e.g., expressed by the robust functional (15a).

The perturbation technique belongs to the simplest sensitivity techniques, in which the first-order derivative is represented by a centered difference approximation for a fixed  $k$ th grid point  $p_m := p_m^{(k)}$ ,  $m = 1, \dots, M$  by [10]

$$\hat{\mathbf{x}}(\mathbf{p}, f) \equiv \frac{\partial \mathbf{x}(\mathbf{p}, f)}{\partial p_m} \doteq \frac{\mathbf{x}(p_m + h, f) - \mathbf{x}(p_m - h, f)}{2h} + \mathcal{O}(h^2). \quad (16)$$

Here,  $h > 0$  is a small value and the notation  $\mathcal{O}(\cdot)$  corresponds to the order of error in the used approximation. The disadvantages of this technique are the computational complexity and an numerical error related to the assumed approximation.

The direct sensitivity analysis, also known as the incremental model technique [5, 19], which can be obtained by differentiating (15b) as follows

$$i\omega \mathbf{C}(\mathbf{p})\hat{\mathbf{x}}(\mathbf{p}, f) + \mathbf{G}(\mathbf{p})\hat{\mathbf{x}}(\mathbf{p}, f) = \underbrace{-i\omega \frac{\partial \mathbf{C}(\mathbf{p})}{\partial p_m} \mathbf{x}(\mathbf{p}, f) - \frac{\partial \mathbf{G}(\mathbf{p})}{\partial p_m} \mathbf{x}(\mathbf{p}, f)}_{\mathbf{j}_{p_m}(f)}. \quad (17)$$

This method, however, requires first forming  $\mathbf{j}_{p_m}(f)$ , i.e., the right-side of (17) and then solving the created system of equations  $M$  times including once analysis of the original problem (15b) in order to evaluate  $\hat{\mathbf{x}}(\mathbf{p}, f)$ . Therefore, this procedure is computationally expansive, even when the LU decomposition is re-used. To improve its numerical efficiency it can be combined with the adjoint variable method [21]. It allows for calculating derivative of the objective function  $F(\mathbf{x}(\mathbf{p}, f))$  in an efficient way by

$$\frac{\partial F(\mathbf{x}(\mathbf{p}, f))}{\partial p_m} := \bar{\mathbf{x}}^\top(\mathbf{p}, f) \mathbf{j}_{p_m}(f), \quad m = 1, \dots, M, \quad (18)$$

where the adjoint variable vector  $\bar{\mathbf{x}}(\mathbf{p}, f)$  is the solution to the adjoint model, defined as

$$i\omega \mathbf{C}(\mathbf{p})\bar{\mathbf{x}}(\mathbf{p}, f) + \mathbf{G}(\mathbf{p})\bar{\mathbf{x}}(\mathbf{p}, f) = (\nabla_{\mathbf{x}} F)^\top \quad (19)$$

with  $\nabla_{\mathbf{x}} F$  denoted as a derivative of  $F(\mathbf{x}(\mathbf{p}, f))$  with respect to the state variable  $\mathbf{x}(\mathbf{p}, f)$  evaluated at the current solution  $\mathbf{x}(\mathbf{p}, f) = \mathbf{x}^*(\mathbf{p}, f)$  [22]. In such a case, this technique becomes a discrete counterpart of a continuous adjoint sensitivity analysis based on Tellegen's theorem [5, 41] or based on the variational approach [7, 14, 26].

Moreover, in case of the robust formulation, the above-described sensitivity techniques can be combined with the PCE (6), (7) and (8) in order to calculate the derivative of mean and of standard deviation [1, 31, 32]. Within this context, in the nanoCOPS project, the variance-based sensitivity analysis (10) has been used in [34] for the solution of a shape optimization problem. In the current work, based on results achieved in [28], the so-called mean gradient sensitivity analysis (12) has been applied to approximate the derivative of the robust functional.

## 5 Results for numerical experiment and discussion

For the purpose of the optimization of the cross-domain coupling under uncertain parameters within a real-life RFIC problem, we replace the EMC, shown on Fig. 1 by the lumped model depicted on Fig. 6. Furthermore, this model has been implemented and simulated in Momentum. The implementation and deterministic simulation have been shown on Figs. 2 and 5, respectively. In our equivalent lumped model, the digital 'dirty' part, that is the aggressor, is represented by a current model  $I_{\text{core}}$  with frequency ranging from 1 MHz to 10 GHz. The resistances treated in the lumped model as deterministic variables are defined in the following way:  $R_1 = 13.2 \text{ } [\Omega]$ ,  $R_2 = 13.2 \text{ } [\Omega]$ ,  $R_3 = 22.7 \text{ } [\Omega]$ ,  $R_4 = 5.6 \text{ } [\Omega]$ ,  $R_{12} = 77 \text{ } [\Omega]$ ,  $R_{13} = 332 \text{ } [\Omega]$ ,  $R_{23} = 217 \text{ } [\Omega]$ ,  $R_{24} = 96 \text{ } [\Omega]$  and  $R_{34} = 130 \text{ } [\Omega]$ . The nominal values of other (deterministic) parameters have been summarized in Table 1.

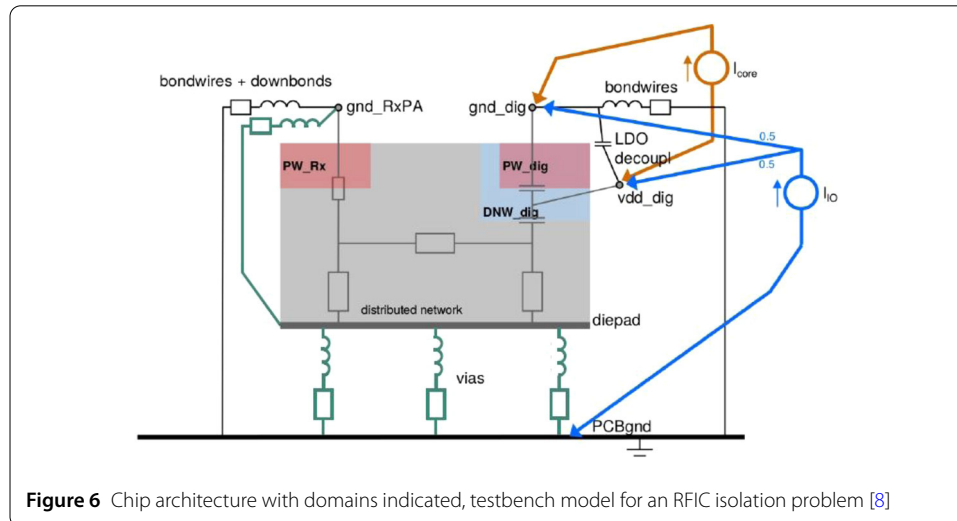
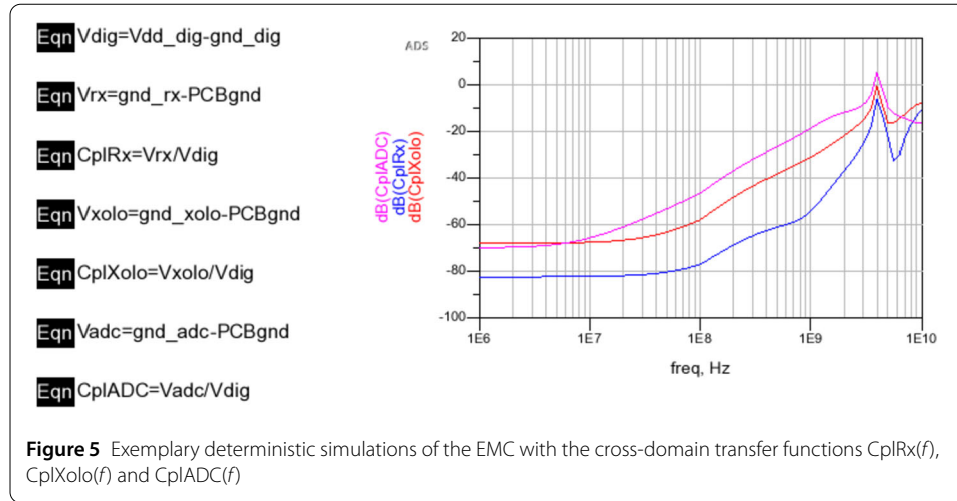


**Table 1** Chosen values for the deterministic elements of the EMC model

	$R_{db}$	$L_{db}$	$R_{bw}$	$L_{bw}$	$C_d$	$C_1$	$C_2$
Elms. values	100.0 [m $\Omega$ ]	0.1 [nH]	100.0 [m $\Omega$ ]	2.0 [nH]	2.3 [nF]	0.4547 [nF]	0.2412 [nF]

**Table 2** The mean values for the initial configuration

	$\bar{R}_{db\_rxpa}^0$	$\bar{L}_{db\_rxpa}^0$	$\bar{R}_{via\_exp}^0$	$\bar{L}_{via\_exp}^0$	$\bar{R}_{lb\_xolo}^0$	$\bar{L}_{lb\_xolo}^0$	$\bar{R}_{lb\_rxpa}^0$	$\bar{L}_{lb\_rxpa}^0$
Mean values	10.0 [m $\Omega$ ]	0.02 [nH]	0.1 [m $\Omega$ ]	0.01 [nH]	20.0 [m $\Omega$ ]	0.4 [nH]	16.7 [m $\Omega$ ]	0.33 [nH]

For the uncertainty quantification, we have chosen four parameters in the form of impedances  $\mathbf{z}(\mathbf{p}) = (z_1(p_1), z_2(p_1), z_3(p_1), z_4(p_1))^T$  with entries defined as  $z_j(p_j) = \bar{R}_j(1 + \delta_j \cdot p_j) + i\omega \bar{L}_j(1 + \delta_j \cdot p_j)$ ,  $j = 1, \dots, J$ ,  $J = 4$  with the magnitude of the perturbation  $\delta_j = 0.2$ . Thus, in our stochastic model to reduce the complexity of the optimization algorithm in terms of the number of iterations, we have made a specific assumption that both parts of the complex number  $z_j$  are perturbed by the same source of noise. The mean values of the random variables have been included in Table 2. Furthermore, the pseudo-

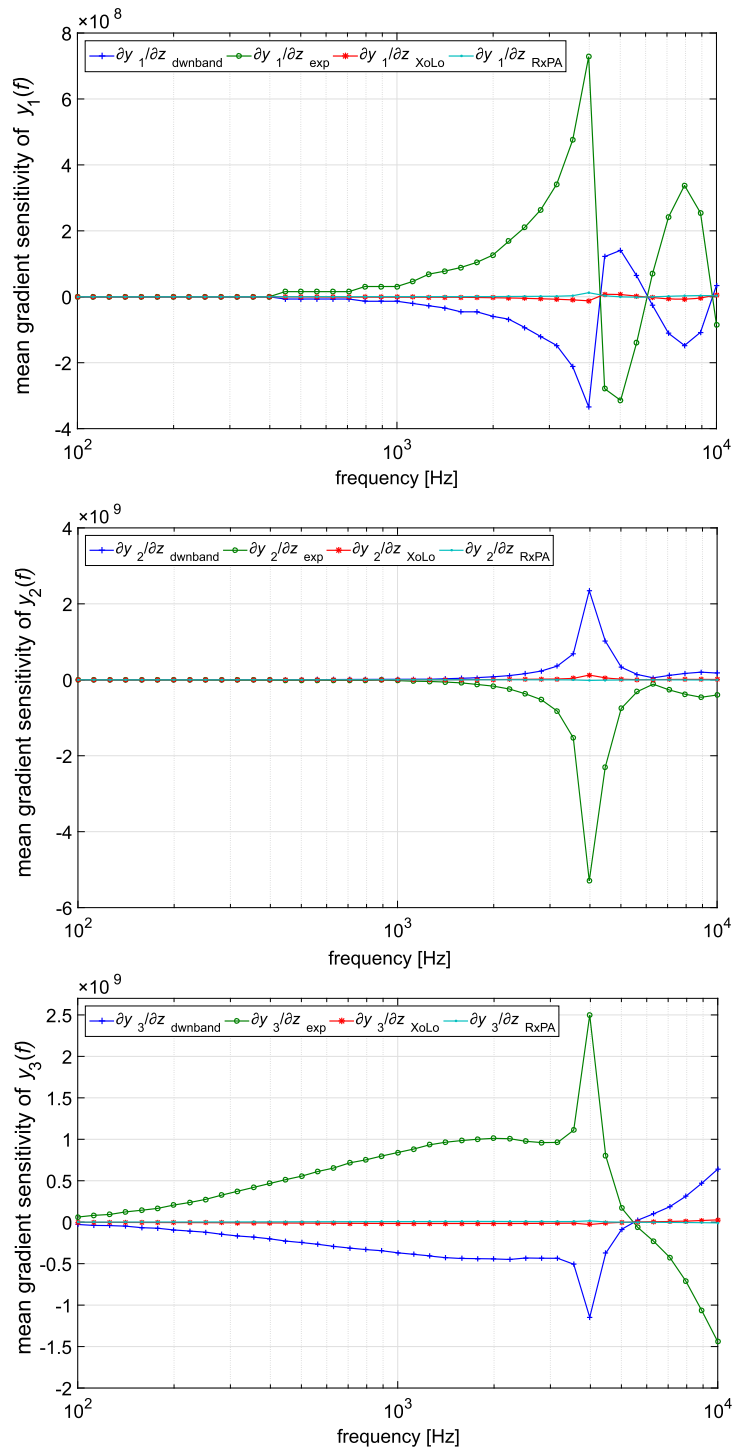


**Figure 7** Mean gradient sensitivity analysis performed for the testbench model. Shown are the means of the coordinates of the gradient of the modulus of the cross-domain frequency response transfer functions  $y_1$ ,  $y_2$  and  $y_3$  with respect to  $\mathbf{p}$



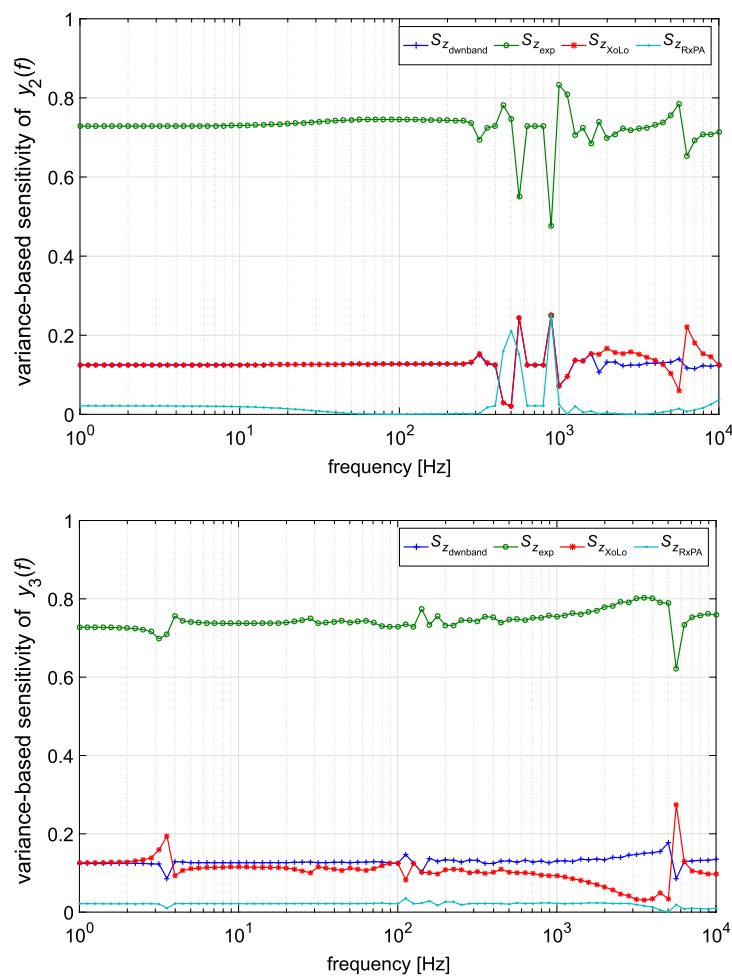


**Figure 8** Variance-based sensitivity performed for the testbench model. Due to the normalization, a value close to 1 means a large ('dominant') contribution to the variance

spectral method for the UQ analysis has been implemented in Python v.2.7.6 using the DAKOTA v.6.2 library [1]. For this purpose, first the set of random parameters  $\mathbf{p}$  and weights  $\mathbf{w}$  have been generated using Stroud 3 quadrature rule. Next, for each quadrature node  $p^k$ ,  $k = 1, \dots, K$ ,  $K = 2J = 8$ , the deterministic simulation of the RFIC model has been run. Due to the application of the uniform distribution for modeling random variables, it holds that  $w_k = 1/8$ . Finally, a priori unknown coefficients of the truncated polynomial chaos have been calculated using (9). The results for the variance-based and mean gradient sensitivity, analyzed in the first iteration of the optimization process, have been depicted on Figs. 8 and 7, respectively.

The algorithm for the robust optimization has been implemented in Octave v.4.0.0 [9] using a scripting language. Thus, the least squares nonlinear optimization problem (15a)–(15c) has been solved in every iteration using the normal equation method and the Tikhonov regularization [27]. The final result of the robust optimization has been presented in Fig. 9, while Table 3 includes the optimized values, found in the 4th iteration. Both the mean values and standard deviations of the cross-domain functions have been reduced considerably, which can be seen on Fig. 9.

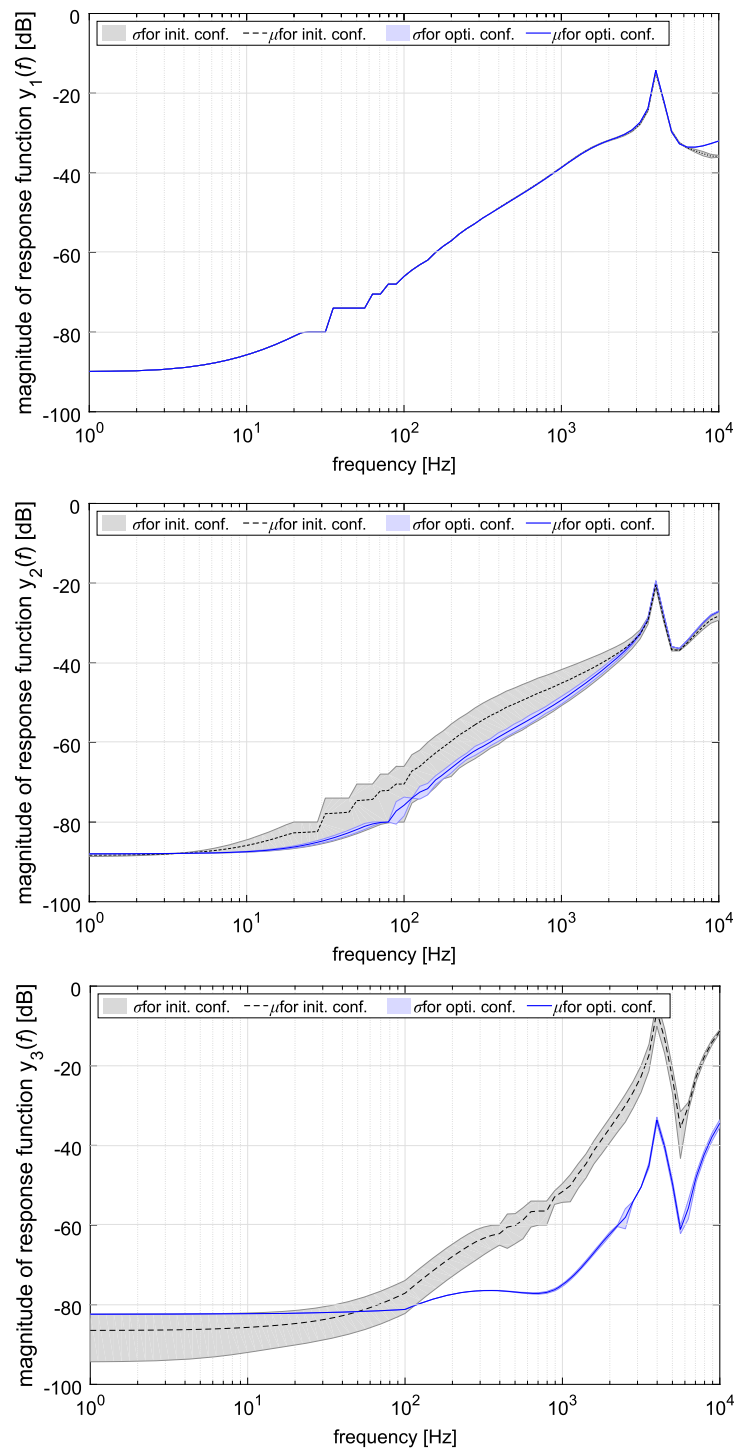


**Figure 9** Result for stochastic optimization of an RFIC problem : mean and standard deviation of the modulus of the cross-domain frequency response transfer functions  $y_1$ ,  $y_2$  and  $y_3$  [28]

## 6 Conclusion

In our work, the PCE-based stochastic collocation method has been applied to study uncertainty propagation throughout the ECM of a real-life RFIC device. In order to reduce

**Table 3** The mean values for the optimized configuration [28]

	$\bar{R}_{db\_rxpa}$	$\bar{L}_{db\_rxpa}$	$\bar{R}_{via\_exp}$	$\bar{L}_{via\_exp}$	$\bar{R}_{lb\_xolo}$	$\bar{L}_{lb\_xolo}$	$\bar{R}_{lb\_rxpa}$	$\bar{L}_{lb\_rxpa}$
Mean values	9.37 [m $\Omega$ ]	0.0187 [nH]	0.13 [m $\Omega$ ]	0.0138 [nH]	25.0 [m $\Omega$ ]	0.5 [nH]	0.36 [m $\Omega$ ]	7.22 [nH]

the computationally expansive simulation of the EMC, we have applied the equivalent lumped model developed by the NXP Semiconductor. It allows for conducting each simulation within the realistic time of about several seconds. Furthermore, based on the response surface model by truncated PCE, it has been possible to provide both the variance-based and local sensitivity analysis of the cross-domain coupling. Thanks to this analysis we could identify the most influential input parameters in a very efficient way. This information can be further used for the physics-based design of an RFIC.

Another effective solution relies in incorporating the UQ into the regularized Gauss-Newton procedure in order to find automatically impedances  $\mathbf{z}$ . This approach applied in our work allows to reduce the coupling effect of  $y_3(f)$  in the mean sense approximately by 27 [dB] across the considered range of frequency (Fig. 9). Also the standard deviation of  $y_2(f)$  and  $y_3(f)$  have been considerably reduced by 90% in average sense.

However, in our opinion, the application of the Pareto front method to solve a multi-objective problem can further improve the provided results for the RFIC interference problem due to competing objective functions  $y_2$  and  $y_3$ . In such a case, the AWM might not approximate properly the Pareto front. However, this issue is considered as a further direction of our research.

#### Acknowledgements

The authors are grateful to the financial support from the European Union in the FP7-ICT-2013-11 Programme.

#### Funding

This FP7 Collaborative Project nanoCOPS is supported by the European Union in the FP7-ICT-2013-11 Programme under Grant Agreement Number 619166 (Project nanoCOPS—nanoelectronic COupled Problems Solutions). For further details see <http://www.fp7-nanocops.eu/>.

#### List of abbreviations

nanoCOPS, Nanoelectronic COupled Problems Solutions; RF, Radio Frequency; RFIC, Radio Frequency Integrated Circuit; SCM, Stochastic Collocation Method; PCE, Polynomial Chaos Expansion; EMI, Electromagnetic Interference; RFCMOS, Radio-Frequency Complementary Metal-Oxide Semi-Conductor; CEM, Computational Electromagnetic; EMC, Electromagnetic Compatibility; IC, Integrated Circuit; ICs, Integrated Circuits; IP, Intellectual Property; UQ, Uncertainty Quantification; ADC, Analog-to-Digital Converter; RxPA, Receiver and Power Amplifier; XoLO, Crystal oscillator and Local Oscillator; IO, Input/Output; IOs, Input/Output systems; PCB, Printed Circuit Board; ECM, Equivalent Circuit Model; ADS, Advanced Design System; MoM, Methods of Moments; PDEs, Partial Differential Equations; MNA, Modified Nodal Analysis; DAEs, Differential-Algebraic Equations; DAC, Digital-to-Analog Converter; VCO, Voltage Controlled Oscillator; PC, Polynomial Chaos; DAKOTA, Design Analysis Kit for Optimization and Terascale Applications.

#### Availability of data and materials

The data that support the findings of this study are available from NXP, but restrictions apply to the availability of these data, which were used under license for the current study, and so are not publicly available.

#### Competing interests

The authors declare that they have no competing interests.

#### Authors' contributions

All authors contributed to the writing of the final version of this paper. However, special merits go to RJ, JN and TB for sharing their experiences from industry, which yielded the development of the methodology for UQ modeling and optimizing of the real-life device; to RP for his work on the UQ; to PP, JtM and MG for their contribution to the robust optimization. All authors read and approved the final version of manuscript.

#### Author details

<sup>1</sup>Bergische Universität Wuppertal, Wuppertal, Germany. <sup>2</sup>Ernst-Moritz-Arndt-Universität Greifswald, Greifswald, Germany.

<sup>3</sup>NXP Semiconductors, Eindhoven, The Netherlands.

**Endnote**

<sup>a</sup> In Fig. 6  $\text{Digital}_{\text{vdd}} = \text{vdd}_{\text{dig}}$ ,  $\text{Digital}_{\text{gnd}} = \text{gnd}_{\text{dig}}$ ,  $\text{RxPA}_{\text{gnd}} = \text{gnd}_{\text{RxPA}}$ ; not found in Fig. 6:  $\text{gnd}_{\text{adc}}$ ,  $\text{XoLO}_{\text{gnd}}$  are mentioned in Fig. 2.

**Publisher's Note**

Springer Nature remains neutral with regard to jurisdictional claims in published maps and institutional affiliations.

Received: 28 March 2018 Accepted: 12 November 2018 Published online: 20 November 2018

**References**

1. Dakota 6.3—algorithms for design exploration and simulation. Albuquerque, NM: Sandia National Laboratories; 2015. <https://dakota.sandia.gov/>.
2. Bruns HD, Schuster C, Singer H. Numerical electromagnetic field analysis for EMC problems. *IEEE Trans Electromagn Compat.* 2007;49(2):253–62.
3. Casper T, De Gersem H, Gotthans T, Schoenmaker W, Schöps S, Wieers A. Electrothermal simulation of bonding wire degradation under uncertain geometries. In: Proceedings of the 2016 design, automation & test in Europe conference & exhibition (DATE); 2016.
4. Chapter SC 47A: integrated circuits. [http://www.iec.ch/emc/emc\\_prod/prod\\_main.htm](http://www.iec.ch/emc/emc_prod/prod_main.htm).
5. Chua LO, Lin PM. Computer aided analysis of electronic circuits: algorithms & computational techniques. Englewood Cliffs: Prentice Hall; 1975.
6. Collin RE. Field theory of guided waves. New York: IEEE Press; 1990.
7. Conway J. A course in functional analysis. New York: Springer; 1997.
8. Di Buccianico A, ter Maten J, Pulch R, Janssen R, Niehof J, Hanssen J, Kapora S. Robust and efficient uncertainty quantification and validation of RFIC isolation. *Radioengineering.* 2014;23:308–18.
9. Eaton JW, Bateman D, Hauberg S, Wehbring R. GNU Octave version 3.8.1 manual: a high-level interactive language for numerical computations. CreateSpace Independent Publishing Platform; 2015. <http://www.gnu.org/software/octave/doc/interpreter>.
10. Eberly D. Derivative approximation by finite differences; 2008. <http://www.geometrictools.com/Documentation/FiniteDifferences.pdf> (last modified: March 2).
11. Feldmann U, Günther M. CAD-based electric-circuit modeling in industry I: mathematical structure and index of network equations. *Surv Math Ind.* 1999;8:97–129.
12. Gharpurey R, Meyer RG. Modeling and analysis of substrate coupling in integrated circuits. *IEEE J Solid-State Circuits.* 1996;31(3):344–53.
13. Günther M, Feldmann U, ter Maten J. Modelling and discretization of circuit problems. In: Ciarlet PG, editor. Handbook of numerical analysis. Vol. 13. Amsterdam: Elsevier; 2005. p. 523–659.
14. Ilievski Z, Xu H, Verhoeven A, ter Maten EJW, Schilders WHA, Mattheij RMM. Adjoint transient sensitivity analysis in circuit simulation. In: Scientific computing in electrical engineering. Berlin: Springer; 2006. p. 183–9. (Mathematics in industry; vol. 11).
15. Kapora S, Hanssen M, Niehof J, Sandifort Q. Methodology for interference analysis during early design stages of high-performance mixed-signal ICs. In: Proceedings of the 2015 10th international workshop on the electromagnetic compatibility of integrated circuits (EMC Compo); 2015. p. 67–71.
16. Koch PN, Yang R-J, Gu L. Design for six sigma through robust optimization. *Struct Multidiscip Optim.* 2004;26:235–48.
17. Marler RT, Arora JS. Survey of multi-objective optimization methods for engineering. *Struct Multidiscip Optim.* 2004;26:369–95.
18. Momentum Keysight Technologies. <http://www.keysight.com/en/>.
19. Nakhla NM, Nakhla M, Achar R. A general approach for sensitivity analysis of distributed interconnects in the time domain. *IEEE Trans Microw Theory Tech.* 2011;59:46–55.
20. Niehof J, van Sinderen J. Preventing RFIC interference issues: a modeling methodology for floorplan development and verification of isolation- and grounding strategies. In: Proceedings of the 2011 15th IEEE workshop on signal propagation on interconnects (SPI); 2011. p. 11–4.
21. Nikolova NK, Bandler JW, Bakr MH. Adjoint techniques for sensitivity analysis in high-frequency structure CAD. *IEEE Trans Microw Theory Tech.* 2004;52:403–19.
22. Nikolova NK, Zhu J, Li D, Bakr MH, Bandler JW. Sensitivity analysis of network parameters with electromagnetic frequency-domain simulators. *IEEE Trans Microw Theory Tech.* 2006;54:670–81.
23. Pulch R, Putek P, De Gersem H, Gillon R. Identification of probabilistic input data for a glue-die-package problem. In: Quintela P, Barral P, Gómez D, Pena FJ, Rodríguez J, Salgado P, Vázquez-Méndez ME, editors. Progress in industrial mathematics at ECMI 2016. Cham: Springer; 2017. (Mathematics in industry; vol. 26).
24. Pulch R, ter Maten EJW, Augustin F. Sensitivity analysis of linear dynamical systems in uncertainty quantification. *Proc Appl Math Mech.* 2013;13:507–8.
25. Pulch R, ter Maten EJW, Augustin F. Sensitivity analysis and model order reduction for random linear dynamical systems. *Math Comput Simul.* 2015;111:80–95.
26. Putek P. Mitigation of the cogging torque and loss minimization in a permanent magnet machine using shape and topology optimization. *Eng Comput.* 2016;33:831–54.
27. Putek P, Crevecoeur G, Slodička M, van Keer R, Van de Wiele B, Dupré L. Space mapping methodology for defect recognition in eddy current testing—type NDT. *Compel.* 2012;31(3):881–94.
28. Putek P, Janssen R, Niehof J, ter Maten EJW, Pulch R, Günther M. Robust optimization of an RFIC isolation problem under uncertainties. In: Scientific computing in electrical engineering. Berlin: Springer; 2018. p. 177–86. (Mathematics in industry; vol. 28).
29. Putek P, Janssen R, Niehof J, ter Maten EJW, Pulch R, Tasić B, Günther M. Nanoelectronic coupled problems solutions: uncertainty quantification of RFIC interference. In: Quintela P, Barral P, Gómez D, Pena FJ, Rodríguez J, Salgado P, Vázquez-Méndez ME, editors. Progress in industrial mathematics at ECMI 2016. Cham: Springer; 2017. (Mathematics in industry; vol. 26).

30. Putek P, Meuris P, Günther M, ter Maten EJW, Pulch R, Wieers A, Schoenmaker W. Uncertainty quantification in electro-thermal coupled problems based on a power transistor device. *IFAC-PapersOnLine*. 2015;48:938–9.
31. Putek P, Meuris P, Pulch R, ter Maten EJW, Günther M, Schoenmaker W, Deleu F, Wieers A. Shape optimization of a power MOS device under uncertainties. In: *Proceedings of the 2016 design, automation & test in Europe conference & exhibition (DATE)*; 2016. p. 319–24.
32. Putek P, Meuris P, Pulch R, ter Maten EJW, Schoenmaker W, Günther M. Uncertainty quantification for robust topology optimization of power transistor devices. *IEEE Trans Magn*. 2016;52:1700104.
33. Putek P, Pulch R, Bartel A, ter Maten EJW, Günther M, Gawrylczyk KM. Shape and topology optimization of a permanent-magnet machine under uncertainties. *J Math Ind*. 2016;6:11.
34. Putek P, ter Maten EJW, Günther M, Sykalski JK. Variance-based robust optimization of a permanent magnet synchronous machine. *IEEE Trans Magn*. 2017;54:8102504.
35. Putek P. Nonlinear magnetoquasistatic interface problem in a PM machine with stochastic PDE constraint. *Eng Optim*. 2018. Accepted for publication.
36. Schwarz DE, Tischendorf C. Structural analysis of electric circuits and consequences for MNA. *Int J Theor Appl*. 2000;28:131–62.
37. Stanisavljević M, Schmid A, Leblebici Y. Reliability of nanoscale circuits and systems: methodologies and circuit architectures. New York: Springer; 2011.
38. Sudret B. Global sensitivity analysis using polynomial chaos expansion. *Reliab Eng Syst Saf*. 2008;93(7):964–79.
39. Sun H, Zhu B, Sun L, Li H, Yang L. EMC computer modelling and simulation of integrated circuit in QFN package. *Prog Electromagn Res M*. 2013;33:263–75.
40. Taguchi G. Taguchi techniques for quality engineering. New York: Quality Resources; 1987.
41. Tellegen BDH. A general network theorem, with applications. *Philips Res Rep*. 1952;7:259–69.
42. Tiesler H, Kirby RM, Xiu D, Preusser T. Stochastic collocation for optimal control problems with stochastic PDE constraints. *SIAM J Numer Anal*. 2012;50:2659–82.
43. Xiu D. Efficient collocation approach for parametric uncertainty analysis. *Commun Comput Phys*. 2007;2:293–309.
44. Xiu D. Numerical methods for stochastic computations—a spectral method approach. Princeton: Princeton University Press; 2010.
45. Xiu D, Hesthaven J. High-order collocation methods for differential equations with random inputs. *SIAM J Sci Comput*. 2005;27(3):1118–39.
46. Xiu D, Karniadakis GE. Modeling uncertainty in steady state diffusion problems via generalized polynomial chaos. *Comput Methods Appl Mech Eng*. 2002;191:4927–48.
47. Yao W, Chen X, Luo W, van Tooren M, Guo J. Review of uncertainty-based multidisciplinary design optimization methods for aerospace vehicles. *Prog Aerosp Sci*. 2011;47:450–79.
48. Yildiz ÖF, Preibisch JB, Niehof J, Schuster C. Sensitivity analysis and empirical optimization of cross-domain coupling on RFICs using polynomial chaos expansion. In: *2017 IEEE international symposium on electromagnetic compatibility & signal/power integrity (EMCSI)*; 2017. p. 102–7.

**Submit your manuscript to a SpringerOpen<sup>®</sup> journal and benefit from:**

- Convenient online submission
- Rigorous peer review
- Open access: articles freely available online
- High visibility within the field
- Retaining the copyright to your article

---

Submit your next manuscript at ► [springeropen.com](https://www.springeropen.com)